A Functioning Chimera of the Cyclic Nucleotide-Binding Domain from the Bovine Retinal Rod Ion Channel and the DNA-Binding Domain from Catabolite Gene-Activating Protein†

Sean-Patrick Scott,‡ Irene T. Weber,‡ Robert W. Harrison,§ Jannette Carey,|| and Jacqueline C. Tanaka*,⊥

Departments of Biology, Chemistry, and Computer Science, Georgia State University, Atlanta, Georgia 30303, Department of Chemistry, Princeton University, Princeton, New Jersey 08544, and Department of Biology, School of Science and Technology, Temple University, Philadelphia, Pennsylvania 19122

Received December 11, 2000; Revised Manuscript Received May 3, 2001

ABSTRACT: The eukaryotic cyclic nucleotide-gated (CNG) ion channels are a family of large membrane proteins activated by cytoplasmic cGMP or cAMP. Their cyclic nucleotide-binding domain is structurally homologous with that of the catabolite gene-activator protein (CAP), a soluble *Escherichia coli* transcription factor. Differences in ligand activation among sensory channels suggest differences in the underlying molecular mechanisms of signal readout. To study the structural, functional, and conformational consequences of nucleotide binding, we fused the cyclic nucleotide-binding domain from the bovine retinal rod CNG channel α subunit (Brα) to the DNA-binding domain from CAP. The chimera forms a soluble dimer that binds both cGMP and cAMP with association constants of 3.7×10^4 M^{-1} for [^{3}H]cGMP and 3.1×10^4 M^{-1} for [^{3}H]cAMP. The binding of cAMP, but not cGMP, exposes a chymotrypsin cleavage site in the chimera at a position similar to the site in the CAP exposed by cAMP binding. At high cAMP concentrations, a biphasic pattern of cleavage is seen, suggesting that the low-affinity cAMP binding sites are also occupied. Cyclic AMP promotes specific binding to a DNA fragment encoding the lac operator region; the K_d for the protein−DNA binding is ∼200 nM, which is 2-fold higher than the K_d for CAP under identical conditions. A 7 Å crystal structure shows that the overall secondary and tertiary structure of Brα/CAP is the same as that of CAP with two cAMP molecules bound per dimer. The biochemical characterization of the chimera suggests it will be a useful system for testing hypotheses about channel activation, providing further insight into channel function.

Cyclic nucleotide-gated (CNG)[1] ion channels were first identified in the primary sensory neurons of the visual (*1*) and olfactory systems (*2*), where they are an integral part of the cascade transducing external stimuli into voltage signals. The phototransduction cascade results in light-induced decreases in cGMP levels in the photoreceptor outer segments (*3*), while cAMP is likely the signal molecule in olfactory cells (*4*, *5*). CNG channels are also expressed in a number of nonsensory cells, including retinal cone terminals (*6*) and ganglion cells (*7*, *8*), cardiac pacemaker cells (*9*), sperm (*10*), and hippocampus (*11*, *12*). The physiological roles of the channels in nonsensory cells, as well as their nucleotide signaling cascades, have yet to be delineated.

Within the CNG channel family, channels respond differently to cGMP and cAMP, which differ only at the C^2 and C^6 positions on the purine ring. Typically, ionic currents are measured from inside-out, excised, patches to determine the nucleotide concentration required for activation of 50% of the current, the $K_{0.5}$, as well as the fraction of current activated at saturation for those nucleotides that are partial agonists. Homotetrameric CNG channels expressed from cDNA encoding the bovine retinal rod α (Brα) subunit are fully activated by cGMP (*13*), while cAMP is a partial agonist (*14*). The olfactory CNG channels, on the other hand, are fully activated by both cGMP and cAMP (*2*, *15*). Since the $K_{0.5}$ values reflect both nucleotide binding and channel gating, it has been difficult to address the molecular basis of nucleotide discrimination in CNG channels. Attempts to measure the direct nucleotide binding to CNG channels have been hampered by the relatively low-affinity binding interaction and the relatively low abundance of the channel protein.

In previous studies, the activation properties of a series of nucleotide analogues were compared (*16*, *17*) and three-dimensional models of the cyclic nucleotide-binding domain were constructed using the coordinates of the cAMP binding

† This work was supported by NIH Grants EY-06640 (J.C.T.) and GM19736 (NRSA to S.-P.S.).

* To whom correspondence should be addressed: Department of Biology, School of Science and Technology, Temple University, Philadelphia, PA 19122. Phone: (215) 204-8868. Fax: (215) 204-6646. E-mail: jtanaka@astro.temple.edu.

‡ Departments of Biology and Chemistry, Georgia State University.

§ Department of Computer Science, Georgia State University.

|| Princeton University.

⊥ Temple University.

[1] Abbreviations: CNG, cyclic nucleotide-gated; cAMP, 3′,5′-cyclic adenosine monophosphate; cGMP, 3′,5′-cyclic guanosine monophosphate; CRP, cAMP receptor protein; CAP, catabolite gene-activator protein; Brα, bovine rod α subunit CNG channel; Brα/CAP, chimera with the bovine rod α CNG channel binding domain (residues 489−604) replacing residues 14−127 of CAP, a S128A mutation, and a histidine tag; SEM, standard error of the mean.

10.1021/bi002804x CCC: $20.00
Published on Web 05/30/2001

domain of the cAMP receptor protein (CAP, also called the cAMP receptor protein or CRP) (*18*, *19*). CAP is a soluble, dimeric, *Escherichia coli* transcription factor activated by the binding of cAMP (*20*, *21*). CAP binds cGMP nearly as well as cAMP, but cGMP does not promote transcription (*22*). Each subunit of 209 residues (*23*−*25*) contains an N-terminal cyclic nucleotide-binding domain and a C-terminal DNA-binding domain (Figure 1B) (*26*). The eight-stranded β barrel of the nucleotide-binding domain is followed by helices B and C, a hallmark of this family of cyclic nucleotide-binding domains. Three conserved glycines (33, 45, and 71), shown in Figure 1C, are important for maintaining the fold of the barrel (*27*). The conserved E72 and R82 interact with the ribofuranose of the cyclic nucleotide (*28*) and are important for binding of the ligand (*29*).

The goal of the work presented here was to express a soluble protein containing the cyclic nucleotide-binding domain of the Brα CNG channel in order to study its ligand activation and signaling properties. We sought an approach that would be capable of providing information about how ligand identity is recognized by the binding domain of the protein and transmitted to a different domain or neighboring subunit. The chimera, Brα/CAP, was constructed from the cyclic nucleotide-binding domain of the Brα CNG channel and the DNA-binding domain of CAP. Our approach was designed to take advantage of the native CAP solubility to minimize the problems of protein folding. The chimeric protein was overproduced by induction in *E. coli* and purified using a histidine tag. No refolding was required. Brα/CAP is a dimer, binds both cAMP and cGMP, and binds DNA specifically at the lac operator in the presence of cAMP. At low resolution, the crystal structure is essentially the same as that of CAP in its overall structure. The chimera undergoes a conformational change exposing a chymotrypsin site upon binding of cAMP but not cGMP. The results demonstrate the utility of this model system for understanding the readout of the ligand signal from the cyclic nucleotide-binding domain of the CNG channel.

MATERIALS AND METHODS

Mutation and PCR Protocols. The cDNAs for CAP and the Brα CNG channel were subcloned into the pAlter-1 vector (Promega) for single-stranded DNA mutagenesis, according to the protocol of Promega. Single-stranded mutagenesis was used to generate a *Sal*I restriction site at the N-terminus of both CAP and the Brα CNG channel cyclic nucleotide-binding domain to swap the domains. Single-stranded mutagenesis was also used to add an *Nde*I restriction site at the start site of the CAP cDNA. The PCR methods of gene splicing by overlap extension (*30*) were used to add the DNA-binding domain of CAP to the cyclic nucleotide-binding domain of Brα and mutate Ser 128 to Ala. The constructs were sequenced after cloning.

The first round of PCR used the cDNA in pAlter-1 plasmids, a 5′ probe for the Brα cDNA of 5′-AGC-AAT-ACA-TGC-ATT-TTC-GAA-ATG-TAA-GCA-AAG-A-3′, and a 3′ CAP probe of 5′-GGT-GAT-AAA-TCA-GTC-TGC-G-3′. The internal probes were 5′-CTT-TCT-CTG-CAT-CTT-TCA-TCA-AAA-TTT-GCT-TCC-3′ for Brα and 5′-TGA-TGA-AAG-ATG-CAG-AGA-AAG-TGG-GCA-ACC-3′ for CAP. The products of the first round were combined with the 5′ Brα probe and the 3′ CAP probe for a second round of PCR. This product was restricted with *Sal*I and *Bss*HII enzymes and the product placed into pAlter-1 with CAP/*Nde*I/*Sal*I similarly restricted. After sequencing had been carried out, the *Nde*I/*Eco*RI fragment of the pAlter-1 CAP/*Nde*I/*Sal*I/PCR fragment was placed into the *Nde*I/*Eco*RI restriction sites of the pET 28a vector for expression.

Protein Expression and Purification. Constructs of Brα/CAP and CAP containing His tags were expressed in the IPTG-inducible vector pET 28a in the BL21(DE3) Lys S cells at 37 °C from Novagen. Four liters of LB medium was inoculated with bacteria, and the bacteria were allowed to grow to an OD_{600} of ∼0.4. At this point, the temperature was decreased to 25 °C. At an OD_{600} of ∼0.6, 0.24 g/L IPTG was added. The cells were allowed to grow for 5 h at 25 °C before harvesting. Cells were spun at 6000 rpm for 15 min in a Sorvall RC-5b refrigerated superspeed centrifuge using a GSA rotor. The pellet was resuspended in binding buffer [20 mM Tris (pH 7.9), 0.5 M NaCl, and 5 mM imidazole] and then sonicated for 1 min on and 1 min off six times at a 30% duty cycle with a power setting of 3 on a Branson model 250 sonifier. The sonicate was centrifuged at 14 000 rpm for 30 min in an SS34 rotor in a Sorvall centrifuge. The resultant supernatant was centrifuged at 35 000 rpm for 90 min in a Ti 60 rotor in a Beckman L8-M ultracentrifuge. For the expression of CAP without a His tag, we followed the previously established procedures (*29*).

The purification of His-tagged Brα/CAP and CAP was accomplished using a Ni^{2+} agarose column from Novagen. After the column was charged and prewashed, the protein was batch loaded onto the column. Following loading, the column was washed with a volume of binding buffer 10 times greater than the bed volume followed by a volume of wash buffer [20 mM Tris (pH 7.9), 0.5 M NaCl, and 60 mM imidazole] 8 times greater than the bed volume. The protein was released from the column in a step with elution buffer [20 mM Tris (pH 7.9), 0.5 M NaCl, and 1 M imidazole]. Protein purification was followed by SDS−PAGE and determination of A_{280}. The fractions containing the purified protein were combined and dialyzed into one of the following buffers and stored at 4 °C: storage buffer [20 mM Tris (pH 7.8), 500 mM NaCl, 0.1 mM EDTA, 0.1 mM DTT, and 50% glycerol], X-ray buffer [50 mM sodium phosphate (pH 8.0), 500 mM NaCl, and 1 mM EDTA], or functional buffer [50 mM Tris (pH 8.0), 500 mM NaCl, and 1 mM EDTA]. Dialysis was performed using a volume that was at least 300 times greater than the sample volume in Pierce Slide-A-Lyzer dialysis cassettes, with a MW cutoff of 10 000. The external buffer was changed at least twice: the first time after 1 h and the second after 4 h. Dialysis was stopped within 16 h. Amicon 10 000 MW cutoff concentrators were used to concentrate the sample. All dialysis and concentration of the protein was carried out at 4 °C. The protein concentration was determined using Bio-Rad protein assay reagent and BSA as a standard. The purification of CAP without a His tag was performed using two steps, following previously published methods (*31*). The first step was ion exchange chromatography using DEAE followed by a BioRex 70 column. The protein was immediately dialyzed into one of the buffers described above.

Cyclic Nucleotide-Binding Assays. Equilibrium binding assays for [^{3}H]cGMP and [^{3}H]cAMP were carried out at

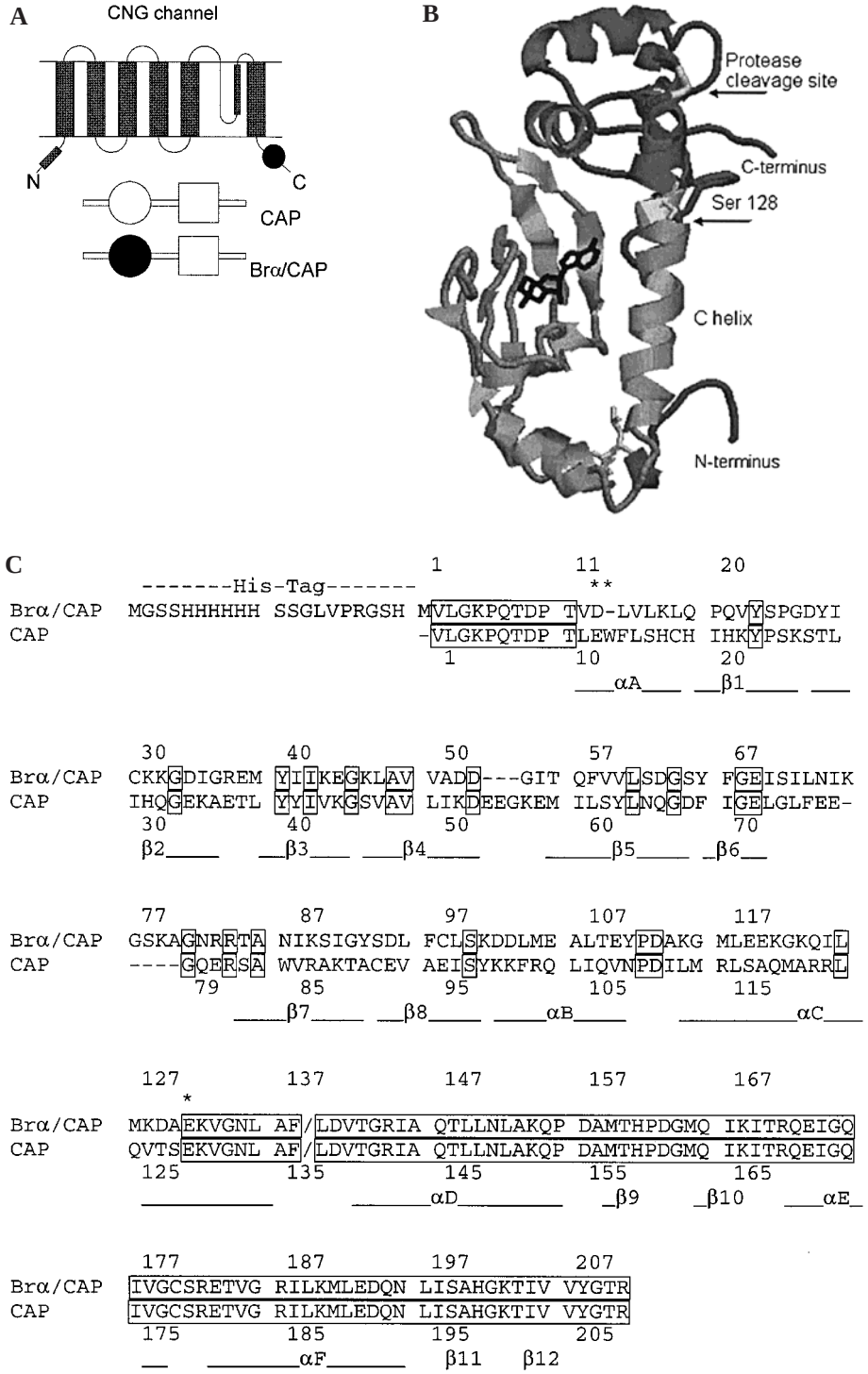

FIGURE 1: (A) Schematic of the Brα/CAP chimera. (Top) The Brα CNG channel consists of cytoplasmic N-terminal and C-terminal regions separated by six transmembrane helices. The pore region is located between transmembrane helices 5 and 6. The C-linker region lies between the final transmembrane segment and the cyclic nucleotide-binding domain (●). (Middle) CAP has an N-terminal cyclic nucleotide-binding domain (○) and a C-terminal DNA-binding domain (□). (Bottom) Brα/CAP protein contains N-terminal residues 1−10 of CAP followed by the Brα CNG channel cyclic nucleotide-binding domain and the DNA-binding domain of CAP. (B) Structure of the CAP monomer. The model was obtained from PDB entry 3GAP. The eight-stranded β barrel cyclic nucleotide-binding domain of CAP (light gray ribbon) is shown at the bottom in this orientation; helix C is labeled. Cyclic AMP is shown as a skeletal model. The DNA-binding domain (dark gray ribbon) lies at the top of this orientation with the protease cleavage site and the S128A mutation indicated by arrows. This picture was generated using RasMol. (C) Sequence of Brα/CAP and CAP. The numbers on the top denote the numbering of Brα/CAP with the histidine tag included. The numbers below the sequence denote CAP residues. The sequence alignment of the Brα portion of Brα/CAP with CAP was described previously (*18*). Identical residues in both CAP and Brα/CAP are boxed. The secondary structure, determined from the CAP−cAMP crystal structure, is shown below the sequences (*26*). A dash denotes the lack of a corresponding amino acid. Amino acids preceding and following the Brα binding domain that do not correspond to either the CAP or CNG channel binding domain are denoted with an asterisk. The slant at position 137 denotes the chymotrypsin cleavage site.

room temperature (20−22 °C) using small Amicon filtration devices. Typically, varying amounts of protein were mixed with ^{3}H-labeled cyclic nucleotides in a total volume of 200 μL containing 50 mM Tris (pH 7.8), 100 mM NaCl, and 1

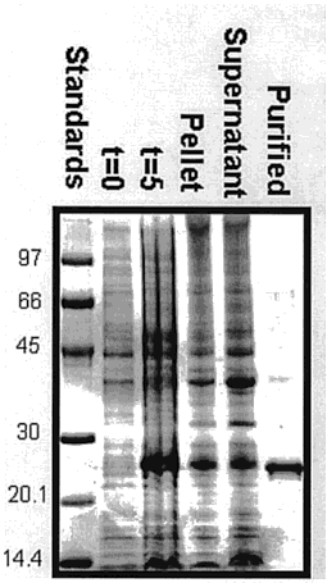

FIGURE 2: Expression of Brα/CAP protein. The Coomassie-stained gel lanes show proteins collected during a typical purification: lane 1, standard MW markers; lane 2, before IPTG induction, at 37 °C; lane 3, after induction for 5 h at 25 °C; lane 4, pellet after 14 000 rpm centrifugation; lane 5, supernatant after 14 000 rpm centrifugation; and lane 6, purified protein following elution from the affinity column.

mM EDTA and allowed to equilibrate for 30 min. Equilibration times were initially based on assays with CAP using 5 min to equilibrate (*32*). Samples were placed into an Amicon centrifugal filter device, with a MW cutoff of 10 000. After 30 min, the sample was spun at 14 000 rpm in a microcentrifuge for 35 s. This allowed approximately 20 μL (10%) of the volume to pass through. Triplicate samples of 5 μL were taken from the top (bound and free ligand) and bottom (free ligand) after centrifugation. Concentration−response data were fitted with a nonlinear algorithm in Tablecurve 4 (Jandel). The binding data shown in Figure 3 were fit with eq 1

$$K_A = \frac{[\text{complex}]}{[\text{Br}\alpha/\text{CAP}][\text{cNMP}]} \quad (1)$$

where Brα/CAP is the concentration of the free chimeric protein, cNMP is the concentration of the free cyclic nucleotide, and K_A is the equilibrium association constant for ligand binding, according to Scheme 1, which assumes one binding site for each monomer of Brα/CAP.

Scheme1

$$\text{Br}\alpha/\text{CAP} + \text{cNMP} \overset{K_A}{\longleftrightarrow} \text{complex}$$

Analytical Ultracentrifugation Experiments. Measurements were taken using a BeckmanXL-I analytical ultracentrifuge. Protein samples were dissolved at approximately 40 μM (monomer) in buffer containing 50 mM Tris, 500 mM NaCl, and 1 mM EDTA (pH 7.8). Sedimentation equilibrium experiments were carried out at 48 000 rpm in six-channel, carbon−epoxy composite centerpieces supplied by Beckman. Equilibrium was assessed by the absence of a significant change in radial concentration gradients in scans separated by a few hours. Data were analyzed by curve fitting to the equation for a single ideal species using Igor-ProÆ (Wavemetrics, Lake Oswego, OR) programs developed from a previous version (*33*). Partial specific volumes and solvent densities were calculated using the program Sedinterp (*34*). We estimate an uncertainty of ±4% in the calculated molecular weight of the protein (*35*). This arises largely from uncertainty in the partial specific volume that is calculated from a weight average of individual amino acids. This degree of accuracy is sufficient to distinguish monomers from aggregates. An alternative model fixed the molecular weight to the value calculated from its sequence and fitted the data to a monomer−dimer equilibrium model.

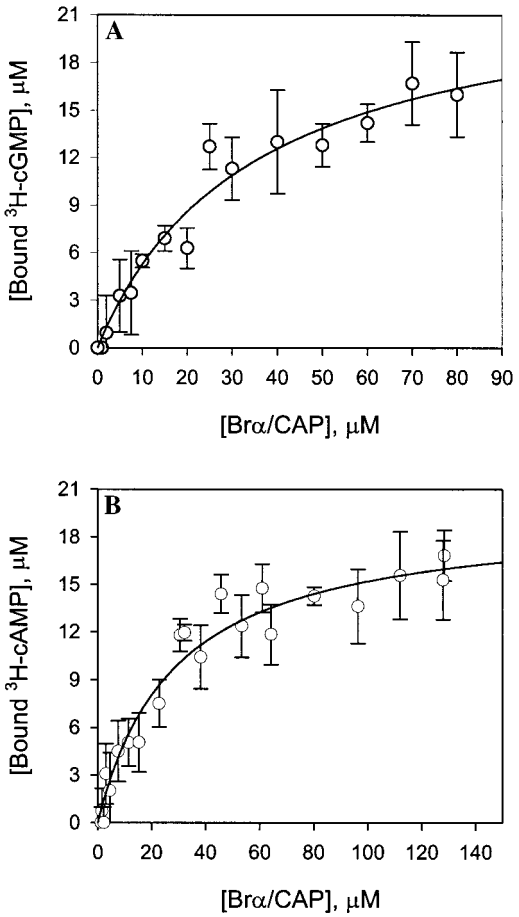

FIGURE 3: Equilibrium binding of [^{3}H]cGMP (A) and [^{3}H]cAMP (B). The level of Brα/CAP binding to [^{3}H]cAMP and [^{3}H]cGMP was determined by rapid partial ultrafiltration (see Materials and Methods) in 50 mM Tris (pH 7.8), 100 mM NaCl, and 1 mM EDTA. The initial ligand concentration was fixed at 20 μM for both cAMP and cGMP. Data points that are shown were fit to eq 1 with the protein concentrations expressed for monomers. The K_A value for [^{3}H]cGMP binding to Brα/CAP was 2.87×10^4 M^{-1}; the saturation value was 24 μM, and the r^2 of the fit was 0.96. The binding to [^{3}H]cAMP gave a K_A of 3.48×10^4 M^{-1} with a saturation of 19.5 μM and an r^2 of 0.96. All binding measurements were made at room temperature (20−21 °C).

Chymotrypsin Proteolytic Assays. The proteolytic assays were performed in the absence of ligand or in the presence of cAMP, cGMP, or other cyclic nucleotides. All assays were performed, following previously described procedures (*36*, *37*), at 37 °C for 30 min in a total volume of 10 μL of the following buffer: 50 mM Tris (pH 7.8), 100 mM NaCl, and 1 mM EDTA. The protein concentration ranged from 0.2 to 0.35 mg/mL, and the chymotrypsin concentration was 12 μg/mL. The proteolysis was stopped by adding the gel

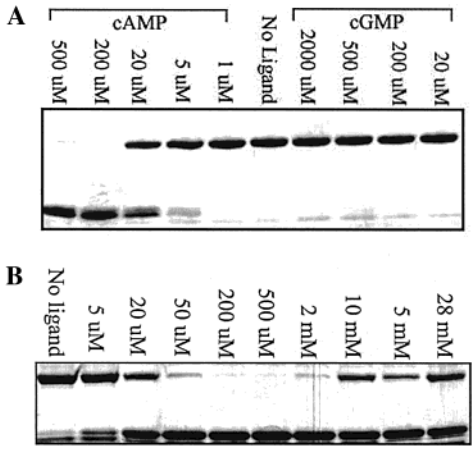

FIGURE 4: Proteolytic cleavage of Brα/CAP. (A) Influence of cyclic nucleotide concentration. Brα/CAP was exposed to chymotryptic digestion for 30 min at 37 °C with the indicated concentration of cyclic nucleotide. Coomassie-stained PAGE gels are shown. The upper band is the intact protein (MW ~ 22500). The lower band (MW ~ 16000) is the proteolyzed fragement containing the cyclic nucleotide-binding domain. (B) Incomplete proteolysis at high concentrations of cAMP. Chymotrypsin digestion was carried out as described for panel A in the presence of the indicated concentrations of cAMP. At cAMP concentrations of >2 mM, partial proteolytic digestion is observed.

loading dye to the sample and heating the samples to >80 °C. If the samples were not immediately loaded onto the gel, they were frozen at −20 °C. All samples were electrophoresed on 10 to 20% SDS−PAGE gels from Owl Separation Systems. Samples were loaded in SDS buffer containing 100 mM Tris (pH 8.8), 200 mM glycine, and 0.1% SDS. Gels were run at ~60 mA for 90 min.

DNA Binding Assay. The lac promoter/operator region DNA was obtained from a pBluescriptII KS plasmid (Stratagene) containing cDNA encoding the catfish olfactory CNG channel (*15*). The plasmid was digested with the *Pvu*II restriction enzyme, and the unresolved fragment mixture was used without further purification. DNA binding was followed the method described by Crothers and co-workers (*38*) with minor modifications. Final solution conditions in the binding reactions were 30 mM sodium acetate, 10 mM Tris-HCl (pH 7.5), 0.1 M NaCl, 10 mM $MgCl_2$, 1 mM DTT, and 10% glycerol. Reaction mixtures 25 μL in volume contained ~3 nM DNA and the indicated concentrations of Brα/CAP or CAP protein. Binding reaction mixtures were incubated at room temperature for 30 min in the presence of 100 μM cAMP, or no nucleotide. Gels of approximately 15 cm × 15 cm × 0.1 cm were composed of 10% (w/v) total acrylamide (29:1 acrylamide:bisacrylamide ratio) and 0.5× TBE buffer (*39*) and were run in 0.5× TBE until a constant current was reached prior to sample loading. Gels initially were run with 20 μM cyclic nucleotide in the gel and recirculating in the running buffer, but identical results were obtained without these additions, as in Figure 4. Samples were loaded while gels were running at 200 V, and then the voltage was reduced to 120 V until the xylene cyanol tracking dye (which comigrates with ~100 bp DNA in this system) had run nearly to the bottom of the gel (~150 min). Gels were stained by soaking in ethidium bromide and photographed under UV illumination.

X-ray Crystallography. Brα/CAP was maintained at a concentration of 4.5 mg/mL in buffer containing 50 mM sodium phosphate, 0.5 M NaCl, 1 mM EDTA (pH 7.8), and 0.5 mM cAMP. This solution was mixed 1:1 with well solution containing 200 mM MES (pH 6.0) and 15% polyethelene glycol 4000 in a hanging drop experiment. X-ray diffraction data were collected on a crystal with dimensions of approximately 0.05 mm × 0.05 mm × 0.1 mm using an R-Axis IIc imaging plate detector mounted on an RU200 Rigaku rotating anode X-ray generator operated at 50 kV and 100 mA with a 0.5 mm collimator. Diffraction data were collected at room temperature with 1.5° oscillations. Each oscillation frame was exposed for 45 min. The distance to the detector plate was set at 100 mm. The diffraction data extended to 7 Å resolution. The data set was merged using the HKL suite (*40*). The space group was determined by symmetry and systematic absences. The diffraction data were reduced in space group $P2_12_12_1$ with the following unit cell dimensions: $a = 105.58$ Å, $b = 98.08$ Å, and $c = 46.70$ Å. The structure was solved by molecular replacement using CCP4 (*41*) with the crystal structure of CAP with cAMP (3GAP) (*28*) as the model. XPLOR (*42*) was used to generate the $2F_o - F_c$ and $F_o - F_c$ maps. The ligand was removed from the 3GAP structure to generate the $(F_o - F_c)_{omit}$ map. The resultant model and maps were visualized using the program CHAIN (*43*).

RESULTS

Construction of Brα/CAP. The CNG channel Brα subunit has 690 amino acids with large cytoplasmic domains on both the N-terminus and C-terminus; six transmembrane helices are positioned between the termini (*44*). Native rod outer segment CNG channels are tetrameric, containing subunits of two types, α and β (*16*, *45*). A schematic of the α subunit is shown in Figure 1A. The pore region lies between the fifth and sixth transmembrane domains. The cyclic nucleotide-binding domain of 120 residues follows the final transmembrane helix (*46*). The Brα/CAP chimera was generated from the cDNA of the α subunit of the bovine rod CNG channel and CAP as shown schematically in Figure 1A. Residues 489−604 of the Brα channel (Brα/CAP residues 14−129 in Figure 1C) replaced residues 14−127 of CAP. The N-terminal start site and the first 10 amino acids of CAP, which lie outside the nucleotide-binding domain, were retained. The swap of Brα for CAP residues was accomplished by introducing a *Sal*I restriction site in the cDNA for both proteins, which changed the DNA sequence of residue L11 in CAP to Val in the chimera, and residue E488 of the Brα binding domain to D12 in the chimera. Following residue D604 in Brα (Brα/CAP residue 129), the native CAP residue S128 at the chimera junction was changed to Ala. Finally, a His tag was added at the N-terminus to facilitate purification.

Expression and Purification of Soluble Brα/CAP. Brα/CAP (Brα/CAP with a His tag) was expressed as a soluble protein following induction with IPTG at 25 °C. In initial experiments with temperature induction, which requires growth at 42 °C (*29*), the majority of the protein was insoluble (data not shown). Typically, IPTG induction following a shift to 25 °C was continued for 5 h. Figure 2 shows the protein gel from a typical purification. Most of the Brα/CAP was present in the soluble fraction (lane 5), although some was present in the insoluble pellet (lane 4) after a 30 min spin at 14 000 rpm. The amount and

distribution of Brα/CAP expressed is roughly equivalent to the amount of His-tagged CAP produced under the same conditions (data not shown). Using a one-step purification with Ni^{2+} agarose, approximately 5 mg of Brα/CAP monomer was obtained per liter of cultured bacteria. The purified protein (lane 6, Figure 2) was ~95% pure.

Both [^{3}H]cAMP and [^{3}H]cGMP Bind to Brα*/CAP*. Initially, [^{3}H]cGMP and [^{3}H]cAMP binding assays were performed by increasing the concentration of the cyclic nucleotide with a fixed amount of Brα/CAP. Complexes were formed in solution containing 100 mM NaCl, 50 mM Tris (pH 7.8), and 1 mM EDTA at room temperature (20−22 °C) and equilibrated for 30 min. Bound and free nucleotides were partially separated by fast centrifugal filtration. The method modifies that reported previously for [^{3}H]cAMP binding to CAP (*47*). In our assay, only a small fraction of the total incubation volume was allowed to pass through the filter, to minimize the potential disturbance of the preexisting equilibrium. The low affinity of the Brα/CAP chimera for cGMP and cAMP resulted in a low signal-to-noise ratio in this assay, especially at high ligand concentrations. The signal-to-noise ratio was improved by using a constant ligand concentration and increasing amounts of protein. Results from such an assay are shown in Figure 3. Fitting of eq 1 assumed one binding site per monomer. More complex models may also fit the binding data, but given the limitations of this assay, we confined our analysis to the simplest model that provided an adequate fit (see the legend of Figure 3). The mean equilibrium association constants from three measurements were $3.72 \times 10^4\ M^{-1} \pm 8.0 \times 10^3$ (SEM) for [^{3}H]cGMP in panel A and $3.09 \times 10^4\ M^{-1} \pm 2.0 \times 10^3$ (SEM) for [^{3}H]cAMP in panel B, indicating that the chimera binds both nucleotides with similar affinities. The limitations of this assay, including its sources of errors, suggest that these values may represent lower limits of the affinities.

Brα/CAP Is a Dimer. Intersubunit interactions in the CAP dimer largely involve residues in the nucleotide-binding domain (*26*). To examine the subunit assembly state of Brα/CAP, sedimentation equilibrium experiments were performed in the analytical ultracentrifuge in the presence and absence of cAMP or cGMP. At a loading concentration of approximately 40 μM, the molecular weight calculated from fitting of a single-species model to the data gives an average molecular weight of 49 000 ± 2000 for Brα/CAP. CAP run under the same conditions without the His tag yielded an average molecular weight of 43 000 ± 2000 (polypeptide molecular weight, 23 509). The observed molecular weight for Brα/CAP corresponds well to twice the calculated molecular weight of the polypeptide (25 315), indicating that the smallest kinetic unit in solution is a dimer in buffer containing 500 mM NaCl, 1 mM EDTA, and 50 mM Tris (pH 7.8) at 25 °C. The ultracentrifugation results also show that the subunit assembly of the chimera does not change upon the binding of ligand. Although the uncertainty in the derived molecular weight is relatively large, the data are not better described by a monomer−dimer equilibrium. Fitting of such a model to the data indicated no more than 5% Brα/CAP monomer at the loading concentration that was used (data not shown). Preliminary analysis of the anisotropy of fluorescently labeled Brα/CAP confirms the presence of dimers even at substantially lower protein concentrations (D. Jameson, S.-P. Scott, and J. Tanaka, unpublished observations).

Proteolysis Reveals cAMP-Induced Conformational Changes. Upon binding cAMP, CAP undergoes conformational changes that expose a chymotrypsin proteolysis site (labeled in panels B and C of Figure 1) between residues 136 and 137 (*36*) to generate two fragments, the cyclic nucleotide-binding domain and the DNA-binding domain. Despite similar binding affinities for cAMP and cGMP, CAP is not cleaved in the presence of cGMP (*37*). In Figure 4A, Brα/CAP was exposed to chymotrypsin in the presence of cGMP and cAMP at different concentrations. At 200 and 500 μM cAMP, the chimera is cleaved in 30 min at 37 °C completely and quantitatively to yield the cyclic nucleotide-binding domain fragment at a molecular weight of approximately 15 000; the smaller DNA-binding domain is not retained on the gels under the running conditions that are used. No cleavage is seen in the absence of ligand or in the presence of cGMP concentrations as high as 2000 μM.

Chymotrypsin digestions were performed at high concentrations of cAMP (Figure 4B). The results show that at cAMP concentrations of ≥5 mM, the conformation of Brα/CAP is partially resistant to proteolysis. Interpretation of this result in light of proteolysis experiments with CAP suggests that the chimera retains the low-affinity cAMP binding sites first seen in the crystal structure of CAP bound to DNA (*48*). These sites are located at the interface of the DNA-binding domain and the nucleotide-binding domain.

The Chimera Binds DNA. CAP is a transcription factor that regulates the expression of multiple genes, including the lac operon, in response to cAMP (*22*). The amino acid sequence of the DNA-binding domain of CAP is not altered in the chimera. To investigate whether Brα/CAP protein also binds DNA, we monitored DNA binding using a gel-retardation assay following methods previously reported for CAP binding (*38*, *49*). A commercially available plasmid (pBluescriptII KS) containing the lac promoter/operator region was used. The plasmid also contained the cDNA encoding the catfish olfactory CNG channel. A *Pvu*II restriction digest of the DNA generated six fragments (121, 152, 300, 592, 1410, and 2450 bp) with the CAP binding site on the 592 bp fragment (arrow in panels A and B of Figure 5). By using the unresolved mixture of fragments, we can assess the selectivity of Brα/CAP for the CAP recognition sequence. Both proteins at different concentrations were incubated with the DNA in the presence or absence of 100 μM cAMP. In the presence of cAMP, both the chimera and CAP bind selectively to the 592 bp fragment of pBluescript KS containing the CAP recognition sequence. Panels A and B of Figure 5 show the results of binding assays carried out with the unresolved mixture of fragments. In lanes 3−6 of panel A, the operator fragment is bound by the chimera in a complex that migrates just below the second largest fragment. Over this range of chimera concentrations, no other fragments are bound, indicating the ability of the chimera to bind specifically to the operator. Similar results are seen for CAP in lanes 4 and 5 of panel B. Under the conditions that were used, the apparent affinities (K_d), estimated from the protein concentration at half-saturation of the DNA, are approximately 100 nM for CAP and 200 nM for the chimera. In the absence of cAMP (panels C and D) or in the presence of cGMP (not shown), both proteins

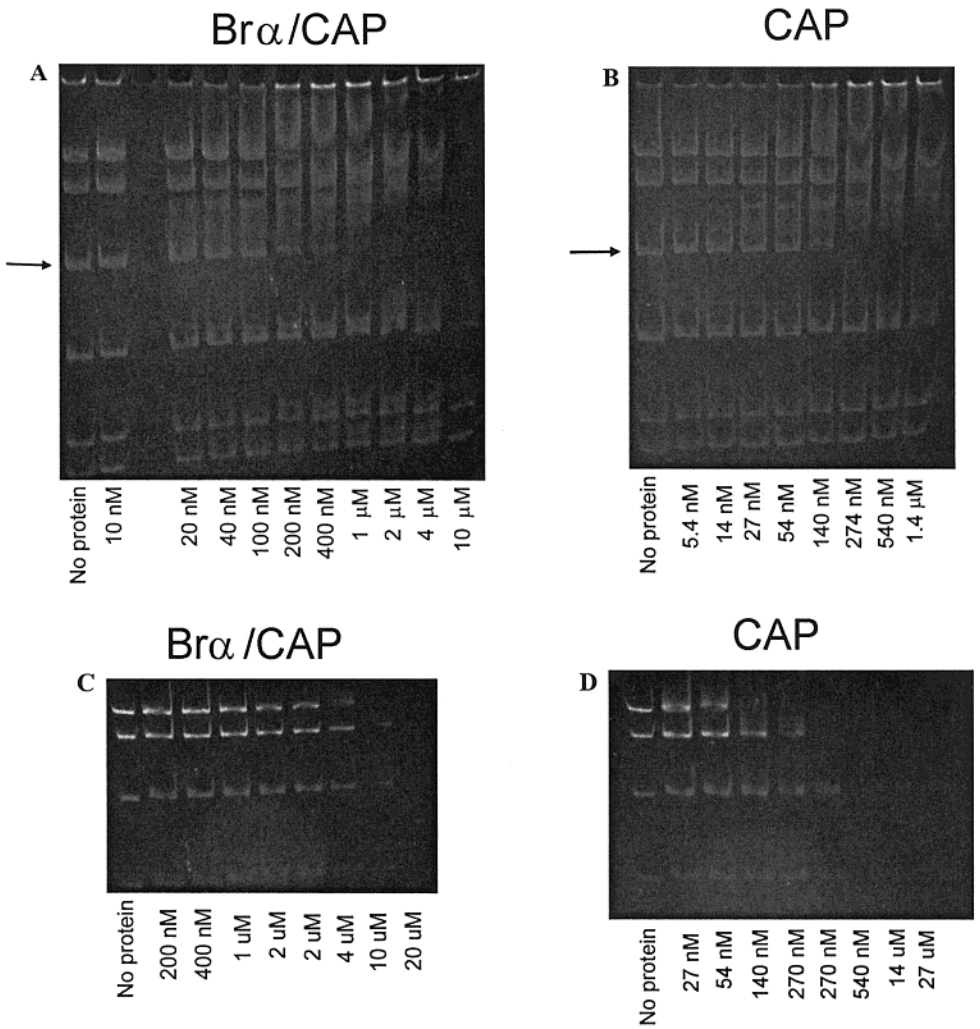

FIGURE 5: DNA binding by Brα/CAP and CAP. Binding reaction mixtures as a function of increasing concentrations of either Brα/CAP (A) or CAP (B) were prepared as described in Materials and Methods in the presence of 100 μM cAMP and resolved on a 10% acrylamide gel. The final protein concentration used in each reaction is indicated by the labels for each lane. DNA was visualized using ethidium bromide. The 592 bp fragment of DNA containing the lac promoter is indicated by the arrow. Reactions identical to those shown in panels A and B (C and D, respectively) were carried out in the absence of cAMP at the indicated protein concentrations.

bind only nonspecifically, with longer fragments bound first. The DNA binding experiments show that Brα/CAP binds to the lac operator sequence of DNA in a cAMP-dependent manner and that the protein−DNA complexes formed with CAP and Brα/CAP have essentially identical mobilities. This result suggests that both bend the DNA to a similar extent. The results also suggest that much of the DNA specificity resides in the DNA-binding domain as expected.

The Structure of Brα/CAP Is Similar to That of CAP. Brα/CAP was crystallized, and diffraction data were obtained to 7 Å resolution. The Brα/CAP unit cell has dimensions (a = 105.58 Å, b = 98.08 Å, and c = 46.70 Å) which are nearly identical to those of the CAP dimer with two cAMP ligands solved in space group $P2_12_12_1$ (*28*). The 849 unique reflections collected to 7.0 Å resolution correspond to 96.3% of the total possible data and exhibited an R_{merge} of 0.148. At this resolution, only the helices are clearly visible. The $2F_o - F_c$ map of the Brα/CAP dimer (not shown) showed cylinders of electron density that correspond to the 12 helices of the CAP dimer, indicating that Brα/CAP is also a dimer with the same overall tertiary structure as CAP. In Figure 7, the $(F_o - F_c)_{omit}$ map using the CAP dimer from which cAMP was removed showed clear difference density at a level of 3σ around two cAMP ligands in the β barrel domain. The difference density peaks are centered on the phosphates of each cAMP. Further, there is no significant difference density at the DNA-binding domains where third and fourth cAMP ligands were shown to bind in a CAP structure cocrystallized with DNA and with cAMP concentrations in the millimolar range (*50*).

DISCUSSION

A molecular characterization of neurotransmitter binding to ion channels and membrane-bound receptors is central to understanding synaptic transmission and signal modulation as well as understanding the molecular basis of many neurological and psychiatric diseases. In our quest to understand cyclic nucleotide communication in CNG channels, we chose the unique approach of inserting the cyclic nucleotide-binding domain from the rod CNG channel into a cAMP-activated bacterial transcription factor. This approach allowed us to avoid some of the limitations of previous studies of soluble neurotransmitter binding domains, namely, problems involving protein folding and solubility, protein expression levels, and readout of ligand signaling. For example, a water-soluble nicotinic acetylcholine receptor

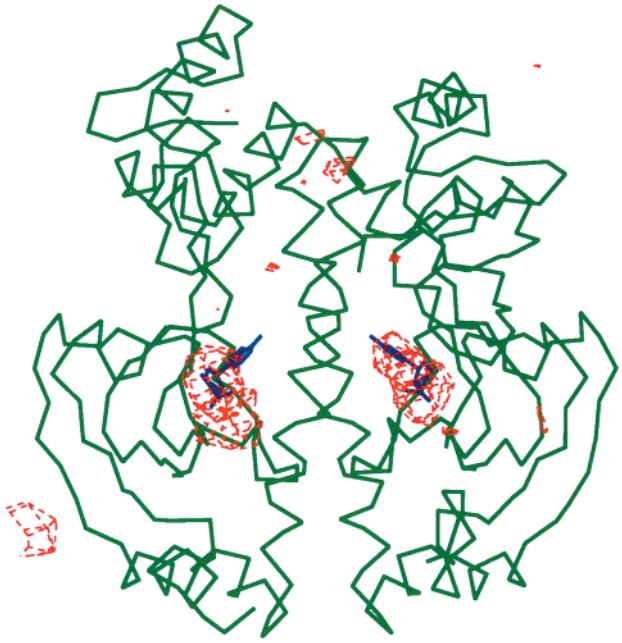

FIGURE 6: Low-resolution structure of Brα/CAP. The X-ray crystal structure of Brα/CAP with cAMP was solved at 7 Å resolution using molecular replacement with PDB entry 3GAP (CAP with two cAMP ligands bound) as the search model. The figure displays the backbone structure of the 3GAP model with the protein in green and the ligands in blue. Superimposed on the model is the $(F_o - F_c)_{omit}$ map density, contoured at the 3σ level (red), obtained using 3GAP with the two cAMP ligands removed.

retaining the α-bungarotoxin binding properties of the native α7 receptor was expressed in *Xenopus* oocytes (*51*). Unfortunately, the yield of the soluble protein was 8 fmol/oocyte, limiting the number of biochemical and biophysical studies than can be done with the protein. In another example, a soluble glutamate receptor, which bound ligands with the characteristic high affinities of the intact receptor, was expressed in bacteria (*52*). The yields were high, but the protein required refolding (*53*, *54*). This construct was used to obtain a high-resolution crystal structure of the ionotrophic glutamate receptor GluR2 (*55*). In comparison, the Brα/CAP chimera does not require refolding, and our purification methods give sufficient yields to study ligand-activated signaling as well as the biochemical and structural properties of the soluble binding domain.

The general assumption of homology modeling is that the three-dimensional folding of functionally related protein domains will be conserved more strongly than the amino acid sequence (*56*). Homology models of several cyclic nucleotide-binding domains based on the structure of CAP provided insight into how cyclic nucleotides interact with the binding domain (*13*, *19*). The structure of the chimera presented here shows that the molecular models based on the 17% level of sequence identity between CAP and Brα nucleotide-binding domains are correct in the overall tertiary fold of the binding domain, although a detailed analysis of the nucleotide interactions must await a high-resolution crystal structure. The ultracentrifugation data and the crystal structure of Brα/CAP offer the first biochemical evidence that the nucleotide-binding domains of two CNG channel subunits interact directly via the long C helices as observed for CAP. This result supports the idea that tetrameric CNG channel assemblies function as a pair of dimers (*57*). The chimera provides a system with which to test directly predictions about nucleotide interactions at the structural and biochemical level, and to correlate the results with the electrophysiology.

The Brα/CAP chimera and CAP share the unusual and unexpected property of binding to cGMP and cAMP with similar affinities despite signaling properties that report the presence of one, but not the other, cyclic nucleotide. CAP binds cAMP with a K_d of ~5 μM and binds cGMP with a 2−6-fold weaker affinity (*22*, *32*, *58*); the binding of cAMP initiates transcription, whereas cGMP has no effect. The chimera binds [^{3}H]cGMP with an affinity of 27 μM and [^{3}H]-cAMP with an affinity of 32 μM. In homomeric Brα channels, cGMP activates maximal currents with a $K_{0.5}$ of ~80 μM, whereas saturating concentrations of cAMP activate ~1% of the maximal current with $K_{0.5}$ values ranging from 800 to 2000 μM (*46*). The $K_{0.5}$ values provide little insight into the relative cyclic nucleotide binding affinities, however, since they reflect the conformational changes involved in channel opening as well as ligand binding (*46*).

Several functional properties of the Brα/CAP chimera examined in this report show clear differences between cGMP and cAMP interactions with the Brα nucleotide-binding domain. In the chymotrypsin assay, cAMP promotes cleavage between the N-terminal nucleotide-binding domain and the C-terminal DNA-binding domain. No proteolytic digestion is seen in the absence of cAMP or in the presence of cGMP. Proteolytic digestion of the chimera as a function of cAMP concentration demonstrates biphasic behavior. This biphasic behavior was reported in chymotrypsin studies with CAP (*36*, *47*), and to understand the behavior, it is necessary to review recent work on CAP which has long been regarded as a paradigm for allosterically activated DNA-binding regulatory proteins (*59*). Exhaustive analysis of its cAMP and DNA binding equilibria aimed at providing a quantitative understanding of allosteric activation led to a widely accepted model that accounts for the biphasic dependence of CAP properties on cAMP concentration (*47*, *58*). In this model, binding of 1 equivalent of cAMP to the CAP dimer suppresses binding of the second cAMP equivalent by negative cooperativity, and activates DNA binding by long-range conformational changes propagated through helix C. Binding of the second cAMP equivalent at much higher cAMP concentrations reduces DNA binding activity. Twenty years of biochemical and biophysical studies on CAP and its mutants were interpreted in terms of this model, and conditions for studying the active form of CAP were determined from it. Then in 1997, a previously undetected second pair of cAMP binding sites was observed in crystals of DNA-bound CAP dimers (*50*). Their location at the crevices between the nucleotide- and DNA-binding domains strongly suggests that cAMP binding to these secondary sites could play a functional role in transcription regulation. Occupancy of the secondary cAMP binding sites at high concentrations of cAMP in CAP has been postulated to account for the biphasic behavior in the chymotrypsin digest (*48*). The cAMP-dependent biphasic pattern seen with Brα/CAP is essentially the same as that seen for CAP, and may have the same underlying explanation for both proteins. The binding pocket for the secondary cAMP sites in the CAP crystal structure of Passner and Steitz (1997) is formed by the bound DNA and by residues of the DNA-binding domain,

principally Q170, Q174, G177, C178, S179, and R180, which are preserved in the chimera, and by residues of the hairpin loop region of CAP, which differ in the chimera. Further studies of both proteins are required to elucidate the basis for their biphasic behaviors.

Differences in cAMP- and cGMP-dependent communication between the Brα nucleotide-binding domain and the DNA-binding domain are also seen in the DNA binding studies. The chimera retains the cAMP-dependent recognition of the lac operator, while cGMP does not promote specific DNA binding. The failure of cGMP to activate transcription in CAP is not understood. To date, all of the CAP structures were obtained with cAMP bound in the cyclic nucleotide-binding domain (*26*, *28*, *50*, *60*−*63*), providing little insight into the cGMP-bound form of CAP or the apo form. The functional assays that have been applied to the chimera to date have been based on assays used for cAMP-activated CAP and thus have not evaluated possible effects of cGMP. Recent studies of CAP show structural and conformational differences upon binding of cGMP versus cAMP (*64*, *65*).

CAP activation by cAMP binding is thought to involve intersubunit communication through the C helices, mediated by the C^6 amino group of cAMP, and rearrangement of the DNA and nucleotide-binding domains via the $\beta4-\beta5$ hairpin loop which lies over the cAMP (*62*). By comparison of the structures of CAP and the CO sensing transcription activator CooA (*66*, *67*), a related CAP family member, the most important regions for allosteric communication were determined to be the C helices and the hairpin loop or switch region corresponding to residues 51−59 in CAP. These residues comprise the loop between $\beta4$ and $\beta5$ and part of the $\beta5$ strand in the Brα channel. Studies of channel activation have generally focused on the interaction between the C helices in the dimer; however, the $\beta4-\beta5$ hairpin region is also likely to be important for transmission of ligand signals as suggested by ligand analogue studies and mutagenesis (*13*, *17*). Although we can only speculate about the role of this critical region in channel activation, future biochemical and biophysical investigations of Brα/CAP will be aimed at resolving ligand-dependent conformational changes in the switch region of Brα.

ACKNOWLEDGMENT

We greatly appreciate the assistance and expertise of Dr. Jim Lear for the ultracentrifugation. We also thank Dr. James Harman for the CAP cDNA clone and Dr. William Zagotta for the cDNA of the α bovine rod CNG channel. We thank Yuan-Fang Wang and Dr. Bhuvaneshwari Mahalingam for assistance and discussions on X-ray experiments. Stacy Stewart and Jason Thomas, undergraduate students in the laboratory, produced the gels shown in Figures 2 and 4.

REFERENCES

1. Fesenko, E. E., Kolesnikov, S. S., and Lyubarsky, A. L. (1985) *Nature 313*, 310−313.
2. Nakamura, T., and Gold, G. H. (1987) *Nature 325*, 442−444.
3. Pugh, E. N., and Lamb, T. D. (1993) *Biochim. Biophys. Acta 1141*, 111−149.
4. Zufall, F., Firestein, S., and Shepherd, G. M. (1994) *Annu. Rev. Biophys. Biomol. Struct. 23*, 577−607.
5. Biel, M., Sautter, A., Ludwig, A., Hofmann, F., and Zong, X. (1998) *Naunyn-Schmiedebergs Arch. Pharmacol. 358*, 140−144.
6. Savchenko, A., Barnes, S., and Kramer, R. H. (1997) *Nature 390*, 694−698.
7. Kawai, F., and Sterling, P. (1999) *J. Neurosci. 19*, 2954−2959.
8. Ahmad, I., Leinders-Zufall, T., Docsis, J. D., Shepherd, G. M., Zufall, F., and Barnstable, C. J. (1994) *Neuron 12*, 155−165.
9. Ludwig, A., Zong, X., Stiebert, J., Hullin, R., Hofmann, F., and Biel, M. (1999) *EMBO J. 18*, 2323−2329.
10. Biel, M., Zong, X., Distler, M., Bosse, E., Klugbauer, N., Murakami, M., Flockerzi, V., and Hofmann, F. (1994) *Proc. Natl. Acad. Sci. U.S.A. 91*, 3505−3509.
11. Kingston, P. A., Zufall, F., and Barnstable, C. J. (1996) *Proc. Natl. Acad. Sci. U.S.A. 93*, 10440−10445.
12. Moosmang, S., Biel, M., Hofmann, F., and Ludwig, A. (1999) *Biol. Chem. 380*, 975−980.
13. Scott, S.-P., and Tanaka, J. C. (1998) *Biochemistry 37*, 17239−17252.
14. Varnum, M. D., Black, K. D., and Zagotta, W. N. (1995) *Neuron 15*, 619−625.
15. Goulding, E. H., Ngai, J., Kramer, R. H., Colicos, S., Axel, R., Siegelbaum, S. A., and Chess, A. (1992) *Neuron 8*, 45−58.
16. Tanaka, J. C., Eccleston, J. F., and Furman, R. E. (1989) *Biochemistry 28*, 2776−2784.
17. Scott, S.-P., and Tanaka, J. C. (1995) *Biochemistry 34*, 2338−2347.
18. Kumar, V. D., and Weber, I. T. (1992) *Biochemistry 31*, 4643−4649.
19. Scott, S.-P., Harrison, R. W., Weber, I. T., and Tanaka, J. C. (1996) *Protein Eng. 9*, 333−344.
20. Zubay, G., Schwatz, D., and Beckwith, J. (1970) *Proc. Natl. Acad. Sci. U.S.A. 66*, 104−110.
21. Emmer, M., de Crombrugghe, B., Pastan, I., and Perlman, R. (1970) *Proc. Natl. Acad. Sci. U.S.A. 66*, 480−487.
22. Anderson, W. B., Perlman, R. L., and Pastan, I. (1972) *J. Biol. Chem. 247*, 2717−2722.
23. Aiba, H., Fujimoto, S., and Ozaki, N. (1982) *Nucleic Acids Res. 10*, 1345−1361.
24. Anderson, W. B., Schneider, A. B., Emmer, M., Perlman, R. L., and Pastan, I. (1971) *J. Biol. Chem. 246*, 5929−5937.
25. Cossart, P., Gicquel-Sanzey, B., and Adhya, S. (1982) *Nucleic Acids Res. 10*, 1363−1378.
26. McKay, D. B., Weber, I. T., and Steitz, T. A. (1982) *J. Biol. Chem. 257*, 9518.
27. Weber, I. T., Steitz, T. A., Bubis, J., and Taylor, S. S. (1987) *Biochemistry 26*, 343−351.
28. Weber, I. T., and Steitz, T. A. (1987) *J. Mol. Biol. 198*, 311−326.
29. Belduz, A. O., Lee, E. J., and Harman, J. G. (1993) *Nucleic Acids Res. 21*, 1827−1835.
30. Horton, R. M., Ho, S. N., Pullen, J. K., Hunt, H. D., Cai, Z., and Pease, L. R. (1993) *Methods Enzymol. 217*, 271−279.
31. Harman, J. G., KcKenney, K., and Peterkofsky, A. (1986) *J. Biol. Chem. 261*, 16332−16339.
32. Donoso-Pardo, J. L., Turner, P. C., and King, R. W. (1987) *Eur. J. Biochem. 168*, 687−694.
33. Brooks, I., Weitzel, R., Chan, W., Lee, G., Watts, D. G., Soneson, K. K., and Hensley, P. (1994) in *Modern Analytical Ultracentrifugation* (Schuster, T. M., and Laue, T. M., Eds.) pp 15−36, Birkhauser, Boston.
34. Laue, T., Shaw, B. D., Ridgeway, T. M., and Pelletier, S. L. (1992) in *Analytical ultracentrifugation in biochemistry and polymer science* (Harding, S. E., Rowe, A. J., and Horton, J. C., Eds.), The Royal Society of Chemistry, Cambridge, U.K.
35. Kharakoz, D. P. (1997) *Biochemistry 36*, 10276−10285.
36. Krakow, J. S., and Pastan, I. (1973) *Proc. Natl. Acad. Sci. U.S.A. 70*, 2529−2533.
37. Ebright, R. H., Le Grice, S. F. J., Miller, J. P., and Krakow, J. S. (1985) *Mol. Biol. 182*, 91−107.
38. Liu-Johnson, H.-N., Gartenberg, M. R., and Crothers, D. M. (1986) *Cell 47*, 995−1005.

39. Maniatis, T., Fritsch, E. F., and Sambrook, J. (1982) in *Molecular cloning. A laboratory manual*, Cold Spring Harbor Laboratory Press, Plainview, NY.
40. Otwinowski, Z., and Minor, W. (1997) in *Methods in Enzymology* (Carter, C. W., and Sweet, R. M., Eds.) Academic Press, San Diego.
41. Collaborative Computational Project Number 4 (1994) *Acta Crystallogr. D50*, 760−763.
42. Brunger, A. T. (1992) *XPLOR*, Yale University Press, New Haven, CT.
43. Sack, J. S. (1988) *J. Mol. Graphics 6*, 224−225.
44. Kaupp, U. B., Niidome, T., Tanabe, T., Terada, S., Bonigk, W., Stuhmer, W., Cook, N. J., Kangawa, K., Matsuo, H., Hirose, T., Miyata, T., and Numa, S. (1989) *Nature 342*, 762−766.
45. Chen, T. Y., Peng, T. W., Dhallan, R. S., Ahamed, B., Reed, R. R., and Yau, K.-W. (1993) *Nature 362*, 764−767.
46. Zagotta, W. N., and Siegelbaum, S. A. (1996) *Annu. Rev. Neurosci. 19*, 235−263.
47. Heyduk, T., and Lee, J. C. (1989) *Biochemistry 28*, 6914−6924.
48. Mukhopadhyay, J., Sur, R., and Parrack, P. (1999) *FEBS Lett. 453*, 215−218.
49. Straney, D. C., Straney, S. B., and Crothers, D. M. (1989) *J. Mol. Biol. 206*, 41−57.
50. Passner, J. M., and Steitz, T. A. (1997) *Proc. Natl. Acad. Sci. U.S.A. 94*, 2843−2847.
51. Wells, G. B., Anand, R., Wang, F., and Lindstrom, J. (1998) *J. Biol. Chem. 273*, 964−973.
52. Arvola, M., and Keinänen, K. (1996) *J. Biol. Chem. 271*, 15527−15532.
53. Chen, G.-Q., and Gouaux, E. (1997) *Proc. Natl. Acad. Sci. U.S.A. 94*, 13431−13436.
54. Chen, G. Q., Sun, Y., Rongsheng, J., and Gouaux, E. (1998) *Protein Sci. 7*, 2623−2630.
55. Armstrong, N., Sun, Y., Chen, G. Q., and Gouaux, E. (2000) *Nature 395*, 913−917.
56. Weber, I. T. (1990) *Proteins: Struct., Funct., Genet. 7*, 172−184.
57. Liu, D. T., Tibbs, G. R., Paoletti, P., and Siegelbaum, S. A. (1998) *Neuron 21*, 235−248.
58. Takahashi, M., Blazy, B., and Baudras, A. (1980) *Biochemistry 19*, 5124−5130.
59. Kolb, A., Busby, S., Buc, H., Garges, S., and Adhya, S. (1993) *Annu. Rev. Biochem. 62*, 749−795.
60. Parkinson, G., Wilson, C., Gunasekera, A., Ebright, Y. W., Ebright, R., and Berman, H. M. (1996) *J. Mol. Biol. 260*, 395.
61. Weber, I. T., Gilliland, G., Harman, J. G., and Peterkofsky, A. (1987) *J. Biol. Chem. 262*, 5630−5636.
62. Passner, J. M., Schulz, S. C., and Steitz, T. A. (2000) *J. Mol. Biol. 304*, 847−859.
63. Schultz, S. C., Shields, G. C., and Steitz, T. A. (1991) *Science 253*, 1001−1007.
64. Won, H. S., Yaazaki, T., Lee, T. W., Yoon, M. K., Park, S. H., Kyogoku, Y., and Lee, B. J. (2000) *Biochemistry 39*, 13953−13962.
65. Baichoo, N., and Heyduk, T. (1999) *Protein Sci. 8*, 518−528.
66. Lanzilotta, W. N., Schuller, D. J., Thorsteinsson, M. V., Kerby, R. L., Roberts, G. P., and Poulos, T. L. (2000) *Nat. Struct. Biol. 7*, 876−880.
67. Chan, M. K. (2000) *Nat. Struct. Biol. 7*, 822.

BI002804X